1   **Pathogenicity and transmissibility of bovine-derived HPAI H5N1 B3.13 virus in pigs**

2

3   Taeyong Kwon [a], Jessie D. Trujillo [a], Mariano Carossino [b, c], Heather M. Machkovech [d], Konner Cool [a], Eu Lim

4   Lyoo [a], Gagandeep Singh [a], Sujan Kafle [a], Shanmugasundaram Elango [a], Govindsamy Vediyappan [a], Wanting Wei [d],

5   Nicholas Minor [e], Franco S. Matias-Ferreyra [a], Igor Morozov [a], Natasha N. Gaudreault [a], Udeni B. R. Balasuriya [b],

6   Lisa Hensley [f], Diego G. Diel [g], Wenjun Ma [h], Thomas C. Friedrich [d, i], Juergen A. Richt [a*]

7

8   **Affiliations**

9   [a] Department of Diagnostic Medicine/Pathobiology, College of Veterinary Medicine, Kansas State University,

10   Manhattan, Kansas, USA

11   [b] Department of Pathobiological Sciences, School of Veterinary Medicine, Louisiana State University, Baton Rouge,

12   Louisiana, USA

13   [c] Louisiana Animal Disease Diagnostic Laboratory, School of Veterinary Medicine, Louisiana State University,

14   Baton Rouge, Louisiana, USA

15   [d] Department of Pathobiological Sciences, University of Wisconsin-Madison, Madison, Wisconsin, USA

16   [e] Department of Pathology and Laboratory Medicine, University of Wisconsin School of Medicine and Public

17   Health, Madison, Wisconsin, USA

18   [f] Zoonotic and Emerging Disease Research Unit, National Bio and Agro-Defense Facility, Agricultural Research

19   Service, United States Department of Agriculture, Manhattan, Kansas, USA

20   [g] Department of Population Medicine and Diagnostic Sciences, College of Veterinary Medicine, Cornell University,

21   Ithaca, New York, USA

22   [h] Department of Veterinary Pathobiology, College of Veterinary Medicine, and Department of Molecular

23   Microbiology and Immunology, School of Medicine, University of Missouri, Columbia, Missouri, USA

24   [i] Wisconsin National Primate Research Center, University of Wisconsin-Madison, Madison, Wisconsin, USA

25

26   [*] Corresponding author: Dr. Juergen A. Richt; email: jricht@ksu.edu

27   **Abstract**

28   Since the first emergence of highly pathogenic avian influenza (HPAI) H5N1 viruses in dairy

29   cattle, the virus has continued to spread, reaching 17 states and at least 970 dairy herds in the

30   United States. Subsequently, spillovers of the virus from dairy cattle to humans have been

31   reported. Pigs are an important reservoir in influenza ecology because they serve as a mixing

32   vessel in which novel reassortant viruses with pandemic potential can be generated. Here, we

33   show that oro-respiratory infection of pigs resulted in productive replication of a bovine-derived

34   HPAI H5N1 B3.13 virus. Infectious virus was mainly identified in the lower respiratory tract of

35   principal infected pigs, and sero-conversion was observed in most of the principal pigs at later

36   time points. In one animal, we detected the emergence of a mutation in hemagglutinin (HA)

37   previously associated with increased affinity for "mammalian-type" $\alpha 2,6$-linked sialic acid

38   receptors, but this mutation did not reach consensus levels. Sentinel contact pigs remained sero-

39   negative throughout the study, indicating lack of transmission. The results support that pigs are

40   susceptible to a bovine-derived HPAI H5N1 B3.13 virus, but this virus did not replicate as

41   robustly in pigs as mink-derived HPAI H5N1 and swine-adapted influenza viruses.

42

43   Keywords: cattle, genotype B3.13, highly pathogenic avian influenza, mammalian-adapting

44   mutation, pathogenicity, pig, transmissibility

Introduction

Highly pathogenic avian influenza (HPAI) viruses have multibasic amino acids in the cleavage site of the HA protein that are recognized by ubiquitous proteases, resulting in systemic disease in poultry [1]. Since the first emergence of A/Goose/Guangdong/1/1996 (Gs/Gd) in 1996, the Gs/Gd lineage of HPAI viruses have sporadically infected humans and caused a 40 to 50% case fatality rate in laboratory-confirmed humans [2]. After continuous evolution, the HA genes of the clade 2.3.4.4b became dominant in HPAI H5 viruses, and spread across the globe via migratory birds, causing HPAI outbreaks in Asia, Europe and North America since 2014 [3,4]. More recently, spillover events of HPAI H5 clade 2.3.4.4b to a variety of mammalian species, especially carnivores and aquatic mammals, have been identified [5]. In early 2024, the first case of HPAI infection in cattle was reported in Texas, United States. Infected dairy cattle exhibited fever, loss of appetite, reduced milk production and poor milk quality [6]. The causative agent was identified as HPAI H5N1 genotype B3.13 virus that was likely the result of a reassortment event between a HPAI H5N1 B3.6 ancestor and North American LPAI viruses [6-8]. On January 2025, a new genotype D1.1 was first detected in bulk milk samples, and trace investigation confirmed HPAI outbreaks caused by D1.1 virus in Nevada dairy farms [9]. As of 2/28/2025, the virus readily spread across the country, affecting 976 dairy herds in 17 states [10]. Moreover, 68 human cases have been reported and the infected humans showed in general mild disease with a single fatal case so far [11]. Most cases were linked to direct exposure to infected cattle (n=41) or poultry (n=24). Experimental studies were immediately performed in cattle to determine the pathogenicity and transmissibility of the newly emerged B3.13 viruses. Experimental infection of lactating cattle via intra-mammary route recapitulated the disease observed in the field, whereas calves infected through intra-nasal and oral routes showed only mild disease with limited virus replication and no transmission to contact sentinels. These findings support the hypothesis that natural infection is established via the intra-mammary route, potentially through the milking process on dairy farms [12,13].

Pigs are natural hosts for H1N1, H1N2, and H3N2 subtypes of influenza A viruses (IAVs) and these viruses readily transmit in pig populations [14]. Sporadic H5N1 infection in pigs has been documented [15,16]. Pigs express sialic acid receptors for both mammalian and avian IAVs in their respiratory epithelium, enabling some avian IAVs to infect pigs [17]. The introduction of

75 avian and human IAVs into swine populations and subsequent reassortment facilitate the

76 expansion of genetic diversity of swine IAVs. Modern agricultural systems and swine exhibitions

77 facilitate spillover events of IAV from swine to humans or vice versa, forming intertwined

78 clusters in phylogenetic trees [18]. Thus, pigs and humans frequently exchange IAV lineages,

79 while pigs are also more susceptible than humans to avian-origin IAVs. Because of this, pigs are

80 thought to serve as mixing vessels in which novel viruses with pandemic potential can be

81 generated [19]. The important role of pigs as the mixing vessel is exampled by the 2009 H1N1

82 pandemic, where the virus underwent reassortment in pigs and acquired novel features and

83 antigenicity to evade the pre-existing immunity in humans [20].

84 Although the current agricultural system enables inter-species transmission of IAV to pigs, the

85 potential of the bovine-derived HPAI H5N1 clade 2.3.4.4b viruses for infection and transmission

86 in pigs remains unclear. Notably, the US first case of H5N1-infected pig was identified in a

87 backyard farm in Oregon, suggesting the expansion of the host range of the contemporary HPAI

88 H5N1 viruses to agricultural animals [21]. Therefore, we aimed to evaluate the pathogenicity and

89 transmissibility of the bovine-derived HPAI H5N1 clade 2.3.4.4b genotype B3.13 virus in pigs.

90

Materials and methods

Viruses and cells

93 Madin-Darby canine kidney (MDCK) cells were maintained in Dulbecco's Modified Eagle

94 Medium (DMEM; Corning, Manassas, VA, USA) supplemented with 5% fetal bovine serum

95 (FBS; R&D systems, Flower Branch, GA, USA) and a 1% antibiotic-antimycotic solution

96 (Gibco, Grand Island, NY, USA). The bovine-derived HPAI H5N1 B3.13 virus,

97 A/Cattle/Texas/063224-24-1/2024, was propagated on bovine uterine epithelial cells (CAL-1; In-

98 house) for 3 passages at Cornell University [6]. At KSU, the virus was propagated on MDCK

99 cells for 1 passage in influenza infection media (DMEM supplemented 0.3% bovine serum

100 albumin, 1% antibiotics- antimycotic solution, 1% non-essential vitamin and 1 µg/mL of TPCK-

101 treated trypsin).

Animal study

103 The animal study and experiments were approved and performed under the Kansas State

104 University (KSU) Institutional Biosafety Committee (IBC, Protocol #1545) and the Institutional

105 Animal Care and Use Committee (IACUC, Protocol #4778) in compliance with the Animal

106 Welfare Act. All animal and laboratory work were performed in a biosafety level-3+ laboratory

107 and BSL-3Ag facility in the Biosecurity Research Institute at KSU in Manhattan, KS, USA

108 except for inactivated samples at BSL-2. Twelve commercial 4-week-old Yorkshire crossbred

109 piglets were obtained from a herd with high health status. Pigs were randomly assigned into

110 principal-infected (n=9) and sentinel (n=3) groups. After acclimation, principals were challenged

111 with 5×10^6 TCID$_{50}$ per pig via intra-tracheal (2 mL), intranasal (1 mL), and oral (1 mL) routes.

112 At 2 day post-challenge (DPC), three sentinels were commingled with principals in a single pen

113 to allow direct contact. Nasal swabs were collected daily until the end of study and

114 oropharyngeal swabs were collected at 1, 3, 5, 7, 10, and 14 DPC. The swabs were resuspended

115 in 2 mL of DMEM supplemented penicillin and streptomycin, filtered using a 0.45µm syringe

116 filter and stored – 80 °C until further analysis. Serum was collected for evaluating antibody

117 responses. Six pigs were randomly selected and humanly euthanized at 3 (n=3, pig ID: #50, #52,

118 and #54) and 5 DPC (n=3, #51, #53, and #61), and the remaining three principals (#57, #59, and

119 #60) and three sentinels (#55, #56, and #58) were humanly euthanized at 14 DPC. At necropsy,

120 bronchoalveolar lavage fluid (BALF) and tissue samples were collected for virological and

121 pathological evaluation.

Virus titration

123 Nasal swab, oropharyngeal swab, BALF and 10% tissue homogenates (w/v) were subjected to

124 virus titration. Clarified or filtered samples were serially diluted in influenza infection media.

125 After washing with 1X PBS, the confluent MDCK cells were inoculated with serially diluted

126 samples. On day 2, the cells were fixed with 100% cold methanol for immunofluorescence assay

127 (IFA) and incubated with the primary antibody (mouse monoclonal antibody HB65, specific for

128 IAV nucleoprotein), and then with anti-mouse IgG conjugated with Alexa Fluor 488 (Invitrogen,

129 Carlsbad, CA, USA). The virus-positive cells were visualized on an EVOS system. The virus

130 titer was determined using the Reed-Muench method.

RNA extraction and Influenza A Matrix-specific RT-qPCR

132   To determine viral RNA shedding and distribution, viral RNA was extracted using a magnetic

133   bead-based automated extraction system (Taco Mini and total nucleic acid extraction kit, Gene

134   Reach, USA) as previously reported [22]. Briefly, nasal swabs, BALF samples and 10% tissue

135   homogenates (DMEM) or formalin fixed tissue homogenates in AL lysis buffer and digested

136   with proteinase K were mixed with an equal volume of the RLT buffer (Qiagen, Germantown,

137   MD, USA) and incubated for 20 minutes at room temperature. Two hundred microliters of the

138   RLT lysate and 200 µL isopropanol were added to the wells containing magnetic beads, followed

139   by 4 sequential washes prior to elution of nucleic acids from the magnetic beads using automated

140   extraction machines (Gene reach Taco Mini or Qiagen Biosprint). RT-qPCR was performed on

141   the Biorad CFX or Opus using a modified version of the NAHLN FLU A matrix detection assay

142   utilizing the qScript XLT 1-Step RT-qPCR ToughMix (QuantaBio, Beverly, MA, USA) [22,23].

143   RT-qPCR was performed in duplicates with a Ct cut-off value of 38. Any samples with Ct>38 or

144   those with positive results on a single replicate were considered suspect positive.

145   **Gross pathology and histopathology**

146   Macroscopic lung lesions were scored, and the percentage of affected pulmonary parenchyma

147   was calculated as previously described [22]. Tissue samples were fixed in 10% neutral buffered

148   formalin, trimmed, processed and stained with hematoxylin and eosin (H&E) following standard

149   procedures. Microscopic pathology was evaluated and scored based on microanatomy of the lung

150   [22]. A minimum of 6 (sentinel animals) and a maximum of 16 (principal-infected animals) lung

151   sections representing all lobes were scored from 0 to 4 (0 = absent, 1 = minimal, 2 = mild,

152   3 = moderate, and 4 = severe) for six separate criteria typically associated with IAV

153   infection in pigs. Scoring categories include (i) epithelial necrosis or attenuation; (ii) airway

154   exudate; (iii) percentage of airways with inflammation; (iv) peribronchiolar and perivascular

155   lymphocytic inflammation; (v) alveolar exudate; (vi) alveolar septal inflammation. For scoring

156   the percentage of airways with inflammation (iii): 0% = 0, up to 10% involvement = 1, 10–

157   39% involvement = 2, 40–69% involvement = 3 and, greater than 70% involvement = 4.

158   Additional tissues from the respiratory tract and lymphoid system were evaluated.

159   **Influenza A virus-specific immunohistochemistry (IHC)**

160   Immunohistochemistry (IHC) for detection of IAV H5N1 nucleoprotein (NP) antigen was

161   performed on the automated BOND RXm platform using the Polymer Refine Red Detection kit

162 (Leica Biosystems, Buffalo Grove, IL) as described previously [22]. The primary antibody

163 (rabbit monoclonal anti-Influenza A virus NP [Cell Signaling Technology, #99797/F8L6X]) was

164 diluted 1:1,200 in Primary Antibody diluent (Leica Biosystems) and incubated for 30 min at

165 ambient temperature. Lung sections from a goose naturally infected with a HPAI H5N1 strain

166 submitted to the Louisiana Animal Disease Diagnostic Laboratory (LADDL) were used as

167 positive assay control.

168 **Serology**

169 The virus neutralization test was performed according to a previously established protocol [24].

170 Briefly, serum samples were heat-inactivated at 56 °C for 30 minutes. A total of 50 µL of a two-

171 fold diluted serum sample was mixed with the equal volume of 100 $TCID_{50}$ of the virus and

172 incubated at 37 °C for 1 hour. After incubation, the mixture was transferred to pre-washed

173 MDCK cells. On day 2, IFA was performed as mentioned above, in order to determine 50%

174 inhibition of virus growth. In addition, commercial NP-based enzyme-linked immunosorbent

175 assay (ELISA) kits, including three competition ELISA kits and one indirect ELISA kit, were

176 used to determine the serological response according to the manufacturers' instruction: (1)

177 AsurDx™ Influenza A virus (IAV) Antibodies cELISA Test Kit, BioStone, USA, (2) ID Screen®

178 Influenza A Nucleoprotein Swine Indirect, Innovative Diagnostics, France, (3) IDEXX Swine

179 Influenza Virus Ab Test, IDEXX, USA and (4) ID Screen® Influenza A Antibody Competition

180 Multi-Species, Innovative Diagnostics, France.

181 **Complementary DNA (cDNA) generation and PCR**

182 We performed reverse transcription, PCR amplification, and library prep as described in the

183 publicly available protocol (https://dx.doi.org/10.17504/protocols.io.kqdg322kpv25/v1). We

184 performed sequencing in two technical replicates, using the same input RNA. We used reagents

185 from the QIAseq DIRECT SARS-CoV-2 Kit A and QIAseq DIRECT SARS-CoV-2 Enhancer

186 (Qiagen). For each sample, we first performed first-strand cDNA synthesis. We assembled a

187 reaction master mix on ice with RP Primer (1 µL), Multimodal RT Buffer (4 µL), RNase

188 Inhibitor (1 µL), nuclease-free water (8 µL), and EZ Reverse Transcriptase (1 µL). We added 5

189 µL of sample RNA to this reaction. The thermal cycling conditions were 25˚C for 10 minutes,

190 42˚C for 10 minutes, 85˚C for 5 minutes, followed by a hold at 4˚C. At this point we also added a

191 no-template control sample consisting of nuclease-free water.

192 Next, cDNA was amplified using a custom primer pool that generates overlapping amplicons of
193 ~250bp. Primer pools was designed as previously described [25]. Briefly, PrimalScheme [26]
194 was used to generate primers from a set of clade 2.3.4.4b, genotype B3.13 H5N1 sequences from
195 the U.S. dairy cattle outbreak (https://github.com/andersen-lab/avian-infuenza). Because
196 sequences including full-length noncoding regions (NCRs) were not available for clade B3.13
197 viruses, we manually designed primers targeting the 5' and 3' termini of each segment. To do this,
198 we inferred likely sequences for the full NCRs of each gene segment based on publicly available
199 sequences of clade 2.3.4.4b H5N1 viruses isolated from North American birds and mammals
200 (https://github.com/moncla-lab/h5-sequencing-protocol-
201 dev/blob/main/RT_and_PCR_protocol.md). Primers targeting the 5' and 3' termini of each
202 segment also included short overhangs not present in the target sequence to enhance
203 amplification efficiency.

204 We used first-strand cDNA from each sample as templated for two independent PCR reactions
205 (one for each primer pool), which we set up using reagents from QIAseq DIRECT SARS-CoV-2
206 Kit A and QIAseq DIRECT SARS-CoV-2 Enhancer. For each PCR reaction we assembled a
207 reaction master mix using 10 µM primer pool (4 µL), 5x UPCR buffer (5 µL), QN Taq
208 Polymerase (1 µL) and nuclease-free water (7 µL). Eight microliters of cDNA were added to
209 each reaction. The cycling conditions were 98˚C for 2 minutes, then 4 cycles of 98˚C for 20
210 seconds and 63˚C for 5 minutes, followed by 29 cycles of 98˚C for 20 seconds and 63˚C for 3
211 minutes with a final hold at 4˚C. A Qubit fluorometer (ThermoFisher) was used to quantify the
212 double-stranded DNA after the reaction.

213 **Oxford Nanopore library prep and sequencing**

214 We prepared libraries according to the protocol for the Oxford Nanopore Technology Native
215 Barcoding Kit V14 (Ligation Sequencing Amplicons - Native Barcoding Kit 96 V14 (SQK-
216 NBD114.96), 2022). The library was sequenced on a minION mk1C sequencer using an R10
217 flow cell.

218 **Processing of the raw sequence data, mapping, variant calling and variant annotation**

219 A bespoke Nextflow pipeline was used to perform Oxford Nanopore base-calling, primer-
220 trimming, and variant-calling (https://github.com/nrminor/oneroof) [27]. The pipeline

221   reproducibly supplies software dependencies via Docker containers, Apptainer containers, or

222   local conda environments built with the Pixi package manager. Base-calling is performed with

223   the Oxford Nanopore Dorado base-caller v0.7.1. Reads are adapter- and primer-trimmed using

224   CutAdapt v4.8 [28]. For the results presented here, we required a minimum read length of 150

225   bases and a maximum read length of 500 bases, along with a minimum average read quality of

226   10. Reads are aligned to the reference genome using minimap2 v2.28, allowing up to 2 primer

227   mismatches between a given primer and the reference sequence [29]. The reference genome used

228   for this piepline is A/Bovine/Texas/24-029328-01/2024 (H5N1), a sequence isolated from an

229   infected cow's milk early in the outbreak [30]. For each gene segment, we manually added the

230   inferred NCR sequences, as well as the synthetic "overhang" sequences present in each primer,

231   to the reference sequence to aid in read mapping. iVar v1.4.2 [31] was used to call variants and

232   snpEff v5.2 [32] was used for variant-effect annotation. Variants were called using a minimum

233   required depth of coverage of 20 reads and a minimum variant frequency of 0.1. Consensus

234   sequences were called using samtools v1.5 [33], with a minimum depth of coverage of 20 and a

235   minimum variant frequency of 0.5.

236   Additional utilities in SeqKit2 v2.8.2 [34], rasusa v2.0.0 [35], vsearch v2.28.1 [36] are used

237   throughout the pipeline, alongside other tools. A full list of the pipeline's dependencies can be

238   found in the GitHub repository's Python project configuration file, "pyproject.toml".

239   **iSNV quality control**

240   VCF files from the Nextflow pipeline were cleaned using a custom R script (R version 4.4.2)

241   [37]. Samples with negative viral titers were removed from downstream analysis. Variants were

242   filtered to include only nonsynonymous and synonymous variants. iSNVs were required to be at

243   a frequency of 0.1 and have a depth of coverage of at least 20 reads. iSNVs were required to be

244   present in both technical replicates with ≥10% frequency based on Grubaugh et al [38]. iSNVs

245   were compared to the GISAID inoculum sequence (accession number EPI_ISL_19155861) [6].

246

247   **Results**

248   In order to determine the pathogenicity and transmissibility of the H5N1 bovine isolate in pigs,

249   animals were challenged with a total of 5×10^6 TCID$_{50}$ intra-orally, intra-nasally and intra-

250   tracheally under experimental settings, and sentinels were co-housed with principals at 2 DPC to

251   allow direct contact (Fig 1A). All principal-infected (n=9) and sentinel (n=3) pigs were active

252   and healthy without apparent clinical signs throughout the study (data not shown). Infectious

253   virus was isolated from nasal swabs of two principal-infected pigs: #50 with 3.16×10^2

254     $TCID_{50}$/mL at 2 DPC and #61 with 2.15×10^4 $TCID_{50}$/mL at 4 DPC and 3.16×10^3 $TCID_{50}$/mL

255   at 5 DPC (Figure 1B). Oropharyngeal swabs of three pigs were found virus-positive at 1 DPC

256   (#52, #59, and #61) and 3 DPC (#52) but the titers were at the limit of detection (Figure 1C). RT-

257   qPCR showed that 7 of 9 principals were positive for viral RNA on at least one time point from 1

258   to 5 DPC in either the nasal or oropharyngeal swabs, suggesting low intermittent shedding

259   (Supplementary figures 1A and 1B). Low levels of infectious virus were isolated from BALF

260   samples of two pigs at 3 DPC (#50 and #52) and other two at 5 DPC (#51 and #61) (Figure 1D).

261   The BALF samples of the virus-negative pigs (#54 at 3 DPC and #53 at 5 DPC) were positive

262   and suspect-positive in RT-qPCR (Supplementary figures 1C and 1D). Low levels of infectious

263   virus was also isolated from lungs of principal-infected pigs: 4.64×10^1 $TCID_{50}$/mL for #50 and

264   #52 at 3 DPC and $1x10^2$ and 4.64×10^1 $TCID_{50}$/mL for #53 and #61 at 5 DPC. One trachea

265   sample (#61) was virus-positive with a titer of 4.64×10^1 $TCID_{50}$/mL at 5 DPC. RT-qPCR data

266   demonstrated that viral RNA was present in multiple respiratory tissues and lymph nodes on 3

267   and 5 DPC, and in one animal in the central nervous system on 5 DPC (Supplementary figures

268   1C and 1D). No infectious virus was isolated from principals at 14 DPC. All swab, BALF, and

269   tissue samples collected from sentinels were negative for virus isolation but a nasal swab and an

270   oral swab of #58 at 4 DPC and 7 DPC, respectively, were suspect positive in RT-qPCR.

271   We next characterized pathological changes in principal-infected pigs at the time of necropsy.

272   Macroscopically, pulmonary lesions in principal-infected pigs (6/6) were characterized by

273   sporadic dark red and depressed lobules representing regions of lobular atelectasis typical of

274   influenza virus A infections primarily at 3 DPC and less frequently at 5 DPC (Figure 2A and

275   supplementary figure 2). Microscopic pulmonary lesions (Figures 2B and 3) consisted of mild to

276   moderate multifocal non-suppurative interstitial pneumonia with rare necrotizing

277   bronchitis/bronchiolitis affecting multiple bronchopulmonary segments. These alterations were

278   mostly comprised of peribronchiolar and perivascular histiocytic and lymphocytic inflammation,

279   extending to and expanding alveolar septa resulting in multifocal areas of consolidation (Figure

280   3A). In the affected bronchopulmonary segments, segmental or individual cellular degeneration

281   and necrosis of the bronchiolar epithelium were noted at 3 DPC (figure 3A and lower right inset)

282   and 5 DPC (Figure 3E upper right inset) in all principal-infected pigs. Intraluminal cell debris

283   and neutrophils were rare. Affected bronchopulmonary segments were rarely accompanied by

284   necrotizing alveolitis (Figure 3A lower left inset), collapse of the alveolar spaces and

285   consolidation of the lobule at 3 DPC and 5 DPC (Figure 3E lower right inset). Areas with

286   bronchiolar and alveolar microscopic changes were also characterized by intracytoplasmic and/or

287   intranuclear viral antigen in bronchial/bronchiolar epithelial cells, pneumocytes and

288   macrophages (3/3 principal-infected pigs at 3DPC; Figures 3B and 3C). At 5 DPC, histologic

289   changes were similar to those occurring at 3DPC in all principal-infected pigs (3/3), with nearly

290   absent bronchial and bronchiolar epithelial cell necrosis (Figures 3E and 3F). Viral antigen was

291   most abundant at 3 DPC and identified in all principal-infected animals (Figures 3B and 3C)

292   with immunolabeling of epithelia (alveolar and bronchiolar). By 5 DPC, viral antigen was

293   present in all principal-infected animals but mostly limited to areas of alveolar/interstitial

294   inflammation (Figure 3G), except in pig #51 and #61 where infrequent bronchiolar epithelial

295   cells were sporadically immunolabeled. At 14 DPC, pulmonary changes were only at the level of

296   the interstitium with multifocal to coalescing areas of mild to rarely moderate, non-suppurative

297   interstitial pneumonia (3/3 principal-infected pigs). Alveolar septa were thickened by infiltrates

298   of lymphocytes and macrophages (Figure 3H and inset) that also expanded interlobular septa

299   (Figures 3H and 3I). Sporadic epithelial cells in bronchioles and alveoli as well as septal

300   macrophages contained viral antigen (Figure 3J and 2/3 principal-infected pigs). Rare individual

301   nasal (3 DPC #54), tracheal and bronchial (3 DPC# 50 and #54, 5 DPC #51 and #61) epithelial

302   cells expressing viral antigen were noted. NP-specific IHC detected individual cellular staining

303   in one or more of the tracheobronchial lymph nodes in all principal-infected pigs (Supplementary

304   figure 3). Lower number of antigen-positive cells and weaker staining intensity were observed at

305   14 DPC, when compared to earlier time points. Rare scattered antigen-positive cells were also

306   detected in the gastro-hepatic lymph nodes from #52 at 3 DPC and #51 at 5 DPC.

307   There were no detectable neutralizing antibodies in the three principals at 7 DPC. Two principal

308   pigs, #59 and #60, were sero-positive with 1:10 VN$_{50\%}$ titer at 10 DPC (Figure 4A). At 14 DPC,

309   neutralizing antibodies were undetectable in serum of #60, but the other two principal pigs (#57

310   and #59) had detectable neutralizing antibodies against H5N1 viruses. Four different ELISA kits,

311   including three NP-based competition ELISA kits and one NP-based indirect ELISA kit,

312   supported clear seroconversion of principal pigs #57 and #59 at 14 DPC but not #60 (Figure 4B

313   and supplementary figure 4). There was no antibody response in any of the sentinel pigs.

314   Collectively, experimental infection led to low levels of antibody responses (#59 and #60) at 10

315   DPC and detectable neutralizing and NP-specific antibody responses in two (#57 and #59) of

316   three principal-infected pigs at 14 DPC.

317   Finally, we asked whether selection might favor the accumulation of additional mammalian-

318   adapting mutations in bovine-derived H5N1 viruses replicating in pigs. We generated viral

319   genome sequences from all samples with sufficient vRNA in technical replicates using a

320   previously described tiled amplicon approach and Oxford Nanopore sequencing (Supplementary

321   figure 5). These sequences were analyzed using a custom pipeline that employs an early cattle

322   isolate, A/Bovine/Texas/24-029328-01/2024, as a standard reference sequence. Note that this

323   reference sequence is slightly different from the isolate used in our inoculations: the original

324   isolate and the virus stock preparation used to inoculate our animals revealed6 mutations relative

325   to this reference sequence. These mutations were maintained at the consensus level in all the

326   specimens from infected pigs, with the exception of one synonymous PB2-A525G (cDNA

327   position), which declined over time below consensus level in some pigs. In addition to these

328   mutations, a total of 11 synonymous and 6 nonsynonymous *de-novo* consensus-level mutations

329   emerged in infected pigs. Five of the 6 *de-novo* nonsynonymous mutations occurred in pig #61,

330   which had the highest viral titers of all the animals (Figure 5). Among these 5 nonsynonymous

331   mutations is an isoleucine-to-methionine substitution at residue 38 of PA (PA-I38M), which was

332   present at the consensus level in nasal swabs from pig #61 at 4 and 5 DPC and is found at sub-

333   consensus levels in other animals (Figure 5). PA-I38M confers resistance to the polymerase

334   inhibitor baloxavir [39]. Another notable consensus-changing nonsynonymous mutation, NA-

335   N307D, was detected in the BALF of #50 at 3 DPC; this mutation may be involved in

336   oseltamivir resistance [39,40]. Several samples also contain viruses harboring HA-D252Y

337   (D236Y in mature H5 numbering and D240Y in H3 numbering); this substitution reached the

338   consensus level in pig #61 oropharyngeal swab at 1 DPC. This residue lies in the HA receptor-

339   binding domain near the 220 loop, but the impact of this particular substitution is not well

340   characterized. One other notable nonsynonymous mutation was HA-S136N (S120N in mature

341   H5 numbering; no directly corresponding amino acid in H3 HA), which was present at 32%

342   frequency in the BALF samples from pig #52 at 3 DPC. This substitution has been shown to

343   increase H5 HA binding to α2,6-linked sialic acids [41]. Also of note, we did not detect

344   emergence of classical mammalian-like mutations in the viral polymerase complex (e.g., PB2-

345   E627K or PB2-D701N) in these pigs, nor did we detect substitutions of other amino acids in HA

346   known to confer effective binding to α2,6-linked sialic acids. Taken together these observations

347   suggest that, although some potentially mammalian-adapting mutations arose in some animals,

348   there is little evidence for extensive additional mammalian adaptation of the bovine-derived

349   HPAI H5N1 B3.13 virus in pigs.

Discussion

351   IAVs exhibit a variety of host tropisms and can cross species barriers. Since HPAI H5 clade

352   2.3.4.4b became dominant in wild bird populations, spillovers to mammalian hosts have been

353   frequently reported worldwide, indicating that viruses possessing the 2.3.4.4b HA may have

354   improved ability to replicate in mammals compared to other HPAI lineages [42]. The outbreak

355   of HPAI H5N1 infection in dairy cattle underscores the potential for clade 2.3.4.4b viruses to

356   emerge in mammals. It is critical to understand the potential for cattle-derived viruses to replicate,

357   evolve, and transmit in pigs, a "mixing vessel" species in which novel reassortant viruses with

358   pandemic potential might be generated. Our study demonstrated limited replication of a bovine-

359   derived HPAI H5N1 B3.13 virus in the upper respiratory tracts of pigs. The limited shedding of

360   virus by principal-infected pigs, in turn, led to no transmission to sentinel pigs even after direct

361   contact, although two samples from sentinel pigs were suspect positive in RT-qPCR, which could

362   be due to cross-contamination in the animal room and/or lab. Rather, the bovine-derived HPAI

363   H5N1 B3.13 virus caused self-limiting infection in pigs with virus replication and pathologic

364   alterations mostly affecting the lower respiratory tract. The low virus titers/viral RNA amounts

365   and low viral antigen presence in the lower respiratory tracts demonstrates inefficient virus

366   replication of the bovine-derived HPAI H5N1 B3.13 virus, when compared to the mink-derived

367   H5N1 clade 2.3.4.4b virus or other swine-adapted IAVs [22,43]. Furthermore, detectable

368   antibody responses were identified in only two out of three principal-infected pigs at 14 DPC.

369   Collectively, our results suggest that pigs are only moderately susceptible to the bovine-derived

370   HPAI H5N1 B3.13 virus.

371   Previous studies have suggested that replication of avian-origin HPAI H5N1 clade 2.3.4.4 viruses

372   are inefficient in the respiratory tracts of pigs [44,45]. In contrast, mammalian isolates of clade

373   2.3.4.4 exhibit higher respiratory pathogenesis in pigs, when compared to avian-origin clade

374   2.3.4.4 viruses, which may be due to the presence of mammalian-adapting mutations in the

375   mammalian isolates. For instance, after experimental infection of pigs with A/Mink/Spain/3691-

376   8_22VIR10586-10/2022, an isolate that showed sustained respiratory transmission among

377   farmed mink and possessed a PB2-T271A mutation, efficient viral replication was identified in

378   the lower respiratory tracts, and neutralizing antibodies were detected in 100% of infected pigs

379   within 7 DPC, albeit no transmission to sentinels was observed [22]. Critical mammalian-like

380   adaptations such PB2-E627K and HA-Q222L (mature H5 numbering) were also detected in

381   mink-adapted H5N1-infected pigs, though these remained at low frequencies [22]. In addition,

382   both the A/raccoon/Washington/22-018406-002/2022 H5N1 virus and the A/redfox/Michigan/22-

383   018712-001/2022 H5N1 virus contained the PB2-E627K substitution , and infection of pigs with

384   these viruses led to pig-to-pig transmission, but the transmission efficiency was low:

385   seroconversion was identified in only 1 out of 5 sentinel pigs after co-mingling with 15

386   principal-infected animals [46]. Although H5N1 viruses isolated from dairy cattle so far mostly

387   lack amino acid substitutions in the polymerase complex previously associated with increased

388   replication in mammalian hosts, such as PB2-E627K and PB2-D701N, they share a different

389   substitution, PB2-M631L, which appears to increase the ability of the polymerase complex to

390   recruit the bovine and human versions of the essential host cofactor ANP32, albeit to a lesser

391   extent than polymerases with PB2-E627K [47]. The PB2-M631L substitution may contribute to

392   the ability of the bovine-derived HPAI H5N1 B3.13 virus to replicate in the respiratory tract of

393   pigs. However, given virus replication kinetics and antibody response, the bovine-derived HPAI

394   H5N1 B3.13 virus was less adapted to the respiratory tract of pigs than the mink-derived HPAI

395   H5N1 virus with the PB2-T271A substitution [22]. Recently, the new genotype D1.1 was also

396   detected in US cattle and characterized as a 4:4 reassortant virus that harbored PB1, HA, M, and

397   NS segments from Eurasian avian lineages and PB2, PA, NP, and NA segments from North

398   American LPAI viruses [9]. Interestingly, the virus retained PB2-D701N mutation that enhances

399   replication in mammalian hosts [48,49], thus the bovine-derived D1.1 virus may present with

400   different replication dynamics in the respiratory tracts of pigs when compared to the bovine-

401   derived B3.13 virus even though the D1.1 virus has not been examined in pigs.

402   We observed few nonsynonymous mutations in the polymerase complex in cattle-derived H5N1

403   viruses replicating in swine. The most notable mutation was PA-I38T, which reached consensus

404 in two specimens from one pig (#61) and was detectable at sub-consensus levels in additional

405 specimens from this and other animals. The PA-I38T substitution is known to confer resistance

406 to the antiviral drug baloxavir and has been observed sporadically in other viruses isolated from

407 infected dairy cattle in the current outbreak. Some previous studies suggest that PA-I38T has

408 minimal costs to viral fitness [50], so it is possible that it can arise and persist in some lineages in

409 the absence of baloxavir selection.

410 In dairy cattle, HPAI H5N1 virus replicates primarily in the mammary tissues and transmission

411 presumably occurs through milk and the milking process. Notably, it is currently understood that

412 bovine mammary tissue mostly expresses "avian-like" α-2,3-linked sialic acid residues [51].

413 Therefore, serial passages in cattle may not incur selective pressures favoring HA mutations that

414 would increase binding to "mammalian-like" α-2,6-linked sialic acids. In the present study, we

415 observed several mutations that could plausibly alter HA receptor-binding preference of the

416 bovine H5N1 virus. We detected HA-D252Y (D236Y in mature H5 numbering) at the consensus

417 level in one sample from pig #61 and at sub-consensus levels in at least one specimen from every

418 other animal except pig #59. Notably, this substitution was also present at a low level in the

419 inoculum, so it is not clear whether its outgrowth in these animals was due to natural selection or

420 genetic drift. However, this residue is within the receptor-binding domain of HA near to the 220

421 loop, which is critical for receptor-binding specificity, so it is possible that D252Y represents a

422 mammal-adapting substitution. We also detected HA-S136N (HA-S120N in mature H5 protein

423 numbering), at 32% frequency in a single sample. This mutation was previously shown to

424 increase the binding of H5 HA to α-2,6-linked sialic acids [41], and could therefore have been

425 favored in the pig respiratory tract; although it is notable that this substitution was detected in

426 BALF and not in an upper respiratory tract sample. It is also notable that mutations predicted to

427 confer α-2,6-linked sialic acid binding have been recently detected at sub-consensus levels in

428 two humans with severe infections caused by H5N1 viruses of the D1.1 genotype [52]. It should

429 be noted that in the present study we tested the early bovine isolate from a milk sample that was

430 collected in February 2024. The dairy cattle outbreak remains ongoing as of February 2025,

431 providing additional opportunities for the emergence of mammalian-like mutations. Therefore, it

432 would be valuable to evaluate the pathogenicity and transmissibility of the latest bovine isolates

433 in mammalian hosts in order to compare the level of adaptation to respiratory tracts of

434 mammalian hosts.

435 In addition to experimental infection of cattle with the bovine-derived HPAI H5N1 B3.13 virus,

436 several groups readily evaluated the pandemic potential of these viruses in well-established

437 animal models. The A/dairy cattle/New Mexico/A240920343-93/2024 strain induced systemic,

438 severe disease in mice after oral ingestion or respiratory infection [53]. Infected ferrets showed

439 clinical signs with systemic viral replication but inefficiently transmitted the virus through the

440 respiratory droplets [53]. Two independent studies supported that the human isolate,

441 A/Texas/37/2024, harboring the PB2-E627K mutation, was more pathogenic and more

442 transmissible than the bovine isolate in ferrets [54,55]. In the primate model, intranasal and

443 intratracheal infection of macaques with A/bovine/OH/B24OSU-342/2024 resulted in mild and

444 severe respiratory disease, respectively, however orogastric inoculation only caused subclinical

445 disease with limited infection and seroconversion [56]. Since the first emergence of the H5N1

446 B3.13 virus in dairy cattle, the virus has been transmitted from cattle to humans with 41

447 confirmed human cases and these humans have experienced mild clinical symptoms, such as

448 conjunctivitis, fever and respiratory symptoms with no hospitalization [57]. In contrast, human

449 infections with D1.1 viruses seem to be more severe resulting in the death of one patient [52,58].

450 Given the severity of clinical outcomes and respiratory tropisms, pigs seem to be better models

451 for the respiratory pathogenesis of HPAI H5N1 clade 2.3.4.4b viruses than mice and ferrets.

452 In summary, our data suggests that pigs are moderately susceptible to the bovine-derived HPAI

453 H5N1 B3.13 virus but do not transmit to sentinel pigs. Given the important role of pigs in IAV

454 ecology as a mixing vessel for generating the novel reassortant viruses with pandemic potential,

455 enhanced surveillance of pigs is warranted.

456

477   **Declaration of interest statement**

478   The J.A.R. laboratory received support from Tonix Pharmaceuticals, Xing Technologies,

479   Esperovax, and Zoetis, outside of the reported work. J.A.R. is inventor on patents and patent

480   applications on the use of antivirals and vaccines for the treatment and prevention of virus

481   infections, owned by Kansas State University.

482

483

484   [1]   Stieneke-Grober A, Vey M, Angliker H, et al. Influenza virus hemagglutinin with
485   multibasic cleavage site is activated by furin, a subtilisin-like endoprotease. EMBO J.
486   1992 Jul;11(7):2407-14.
487   [2]   World Health Organization. Cumulative number of confirmed human cases for avian
488   influenza A(H5N1) reported to WHO, 2003-2023, 5 January 2023. 2023.
489   [3]   WHO/OIE/FAO H5N1 Evolution Working Group. Toward a unified nomenclature system
490   for highly pathogenic avian influenza virus (H5N1). Emerg Infect Dis. 2008 Jul;14(7):e1.
491   [4]   World Health Organization. Evolution of the influenza A(H5) haemagglutinin:
492   WHO/OIE/FAO H5 Working Group reports a new clade designated 2.3.4.4 2015.
493   Available from: https://www.who.int/publications/m/item/evolution-of-the-influenza-
494   a(h5)-haemagglutinin-who-oie-fao-h5-working-group-reports-a-new-clade-designated-
495   2.3.4.4
496   [5]   Adlhoch C, Fusaro A, Gonzales JL, et al. Avian influenza overview April - June 2023. EFSA
497   J. 2023 Jul;21(7):e08191.

498 [6]   Caserta LC, Frye EA, Butt SL, et al. Spillover of highly pathogenic avian influenza H5N1
499   virus to dairy cattle. Nature. 2024 Jul 25.
500 [7]   Nguyen T-Q, Hutter C, Markin A, et al. Emergence and interstate spread of highly
501   pathogenic avian influenza A(H5N1) in dairy cattle. bioRxiv. 2024.
502 [8]   Peacock TP, Moncla L, Dudas G, et al. The global H5N1 influenza panzootic in mammals.
503   Nature. 2025 Jan;637(8045):304-313.
504 [9]   Animal and Plant Health Inspection Service. The Occurrence of Another Highly
505   Pathogenic Avian Influenza (HPAI) Spillover from Wild Birds into Dairy Cattle.
506   https://www.aphis.usda.gov/sites/default/files/dairy-cattle-hpai-tech-brief.pdf2025.
507 [10] Centers for Disease Control and Prevention. HPAI Confirmed Cases in Livestock 2025.
508   Available from: https://www.aphis.usda.gov/livestock-poultry-disease/avian/avian-
509   influenza/hpai-detections/hpai-confirmed-cases-livestock
510 [11] Centers for Disease Control and Prevention. H5 Bird Flu: Current Situation 2024.
511   Available from: https://www.cdc.gov/bird-flu/situation-summary/index.html#human-
512   cases
513 [12] Baker AL, Arruda B, Palmer MV, et al. Dairy cows inoculated with highly pathogenic avian
514   influenza virus H5N1. Nature. 2024 Oct 15.
515 [13] Halwe NJ, Cool K, Breithaupt A, et al. H5N1 clade 2.3.4.4b dynamics in experimentally
516   infected calves and cows. Nature. 2024 Sep 25.
517 [14] Ma W, Vincent AL, Lager KM, et al. Identification and characterization of a highly virulent
518   triple reassortant H1N1 swine influenza virus in the United States. Virus Genes. 2010
519   Feb;40(1):28-36.
520 [15] Nidom CA, Takano R, Yamada S, et al. Influenza A (H5N1) viruses from pigs, Indonesia.
521   Emerg Infect Dis. 2010 Oct;16(10):1515-23.
522 [16] Choi YK, Nguyen TD, Ozaki H, et al. Studies of H5N1 influenza virus infection of pigs by
523   using viruses isolated in Vietnam and Thailand in 2004. J Virol. 2005 Aug;79(16):10821-5.
524 [17] Ito T, Couceiro JN, Kelm S, et al. Molecular basis for the generation in pigs of influenza A
525   viruses with pandemic potential. J Virol. 1998 Sep;72(9):7367-73.
526 [18] Anderson TK, Chang J, Arendsee ZW, et al. Swine Influenza A Viruses and the Tangled
527   Relationship with Humans. Cold Spring Harb Perspect Med. 2021 Mar 1;11(3).
528 [19] Scholtissek C. Molecular evolution of influenza viruses. Virus Genes. 1995;11(2-3):209-
529   15.
530 [20] Mena I, Nelson MI, Quezada-Monroy F, et al. Origins of the 2009 H1N1 influenza
531   pandemic in swine in Mexico. Elife. 2016 Jun 28;5.
532 [21] Animal and Plant Health Inspection Service. Federal and State Veterinary Agencies Share
533   Update on HPAI Detections in Oregon Backyard Farm, Including First H5N1 Detections in
534   Swine. https://www.aphis.usda.gov/news/agency-announcements/federal-state-
535   veterinary-agencies-share-update-hpai-detections-oregon2024.
536 [22] Kwon T, Trujillo JD, Carossino M, et al. Pigs are highly susceptible to but do not transmit
537   mink-derived highly pathogenic avian influenza virus H5N1 clade 2.3.4.4b. Emerg
538   Microbes Infect. 2024 Dec;13(1):2353292.
539 [23] Sponseller BA, Strait E, Jergens A, et al. Influenza A pandemic (H1N1) 2009 virus
540   infection in domestic cat. Emerg Infect Dis. 2010 Mar;16(3):534-7.

541   [24]   Gauger PC, Vincent AL. Serum Virus Neutralization Assay for Detection and Quantitation
542   of Serum Neutralizing Antibodies to Influenza A Virus in Swine. Methods Mol Biol.
543   2020;2123:321-333.
544   [25]   Lail AJ, Vuyk WC, Machkovech H, et al. Pasteurized retail dairy enables genomic
545   surveillance of H5N1 avian influenza virus in United States cattle. medRxiv. 2024.
546   [26]   Quick J, Grubaugh ND, Pullan ST, et al. Multiplex PCR method for MinION and Illumina
547   sequencing of Zika and other virus genomes directly from clinical samples. Nat Protoc.
548   2017 Jun;12(6):1261-1276.
549   [27]   Di Tommaso P, Chatzou M, Floden EW, et al. Nextflow enables reproducible
550   computational workflows. Nat Biotechnol. 2017 Apr 11;35(4):316-319.
551   [28]   Martin M. Cutadapt removes adapter sequences from high-throughput sequencing
552   reads. EMBnetjournal. 2011;17(1).
553   [29]   Li H. Minimap2: pairwise alignment for nucleotide sequences. Bioinformatics. 2018 Sep
554   15;34(18):3094-3100.
555   [30]   Burrough ER, Magstadt DR, Petersen B, et al. Highly Pathogenic Avian Influenza A(H5N1)
556   Clade 2.3.4.4b Virus Infection in Domestic Dairy Cattle and Cats, United States, 2024.
557   Emerg Infect Dis. 2024 Jul;30(7):1335-1343.
558   [31]   Castellano S, Cestari F, Faglioni G, et al. iVar, an Interpretation-Oriented Tool to Manage
559   the Update and Revision of Variant Annotation and Classification. Genes (Basel). 2021
560   Mar 8;12(3).
561   [32]   Cingolani P, Platts A, Wang le L, et al. A program for annotating and predicting the effects
562   of single nucleotide polymorphisms, SnpEff: SNPs in the genome of Drosophila
563   melanogaster strain w1118; iso-2; iso-3. Fly (Austin). 2012 Apr-Jun;6(2):80-92.
564   [33]   Danecek P, Bonfield JK, Liddle J, et al. Twelve years of SAMtools and BCFtools.
565   Gigascience. 2021 Feb 16;10(2).
566   [34]   Shen W, Sipos B, Zhao L. SeqKit2: A Swiss army knife for sequence and alignment
567   processing. Imeta. 2024 Jun;3(3):e191.
568   [35]   Hall M. Rasusa: Randomly subsample sequencing reads to a specified coverage. Journal
569   of Open Source Software. 2022;7(69).
570   [36]   Rognes T, Flouri T, Nichols B, et al. VSEARCH: a versatile open source tool for
571   metagenomics. PeerJ. 2016;4:e2584.
572   [37]   R Core Team. R: A Language and Environment for Statistical Computing. R Foundation for
573   Statistical Computing. https://www.R-project.org/. 2024.
574   [38]   Grubaugh ND, Gangavarapu K, Quick J, et al. An amplicon-based sequencing framework
575   for accurately measuring intrahost virus diversity using PrimalSeq and iVar. Genome Biol.
576   2019 Jan 8;20(1):8.
577   [39]   Nguyen HT, Chesnokov A, De La Cruz J, et al. Antiviral susceptibility of clade 2.3.4.4b
578   highly pathogenic avian influenza A(H5N1) viruses isolated from birds and mammals in
579   the United States, 2022. Antiviral Res. 2023 Sep;217:105679.
580   [40]   Stoner TD, Krauss S, DuBois RM, et al. Antiviral susceptibility of avian and swine
581   influenza virus of the N1 neuraminidase subtype. J Virol. 2010 Oct;84(19):9800-9.
582   [41]   Wang W, Lu B, Zhou H, et al. Glycosylation at 158N of the hemagglutinin protein and
583   receptor binding specificity synergistically affect the antigenicity and immunogenicity of

584   a live attenuated H5N1 A/Vietnam/1203/2004 vaccine virus in ferrets. J Virol. 2010
585   Jul;84(13):6570-7.

586 [42] World Health Organization. Assessment of risk associated with recent influenza A(H5N1)
587   clade 2.3.4.4b viruses. 2022.

588 [43] Kwon T, Artiaga BL, McDowell CD, et al. Gene editing of pigs to control influenza A virus
589   infections. Emerg Microbes Infect. 2024 Jul 31:2387449.

590 [44] Kaplan BS, Torchetti MK, Lager KM, et al. Absence of clinical disease and contact
591   transmission of HPAI H5NX clade 2.3.4.4 from North America in experimentally infected
592   pigs. Influenza Other Respir Viruses. 2017 Sep;11(5):464-470.

593 [45] Graaf A, Piesche R, Sehl-Ewert J, et al. Low Susceptibility of Pigs against Experimental
594   Infection with HPAI Virus H5N1 Clade 2.3.4.4b. Emerg Infect Dis. 2023 Jul;29(7):1492-
595   1495.

596 [46] Arruda B, Baker ALV, Buckley A, et al. Divergent Pathogenesis and Transmission of Highly
597   Pathogenic Avian Influenza A(H5N1) in Swine. Emerg Infect Dis. 2024 Apr;30(4):738-751.

598 [47] Dholakia V, Quantrill JL, Richardson S, et al. Polymerase mutations underlie early
599   adaptation of H5N1 influenza virus to dairy cattle and other mammals. bioRxiv. 2025.

600 [48] Li Z, Chen H, Jiao P, et al. Molecular basis of replication of duck H5N1 influenza viruses in
601   a mammalian mouse model. J Virol. 2005 Sep;79(18):12058-64.

602 [49] Gao Y, Zhang Y, Shinya K, et al. Identification of amino acids in HA and PB2 critical for the
603   transmission of H5N1 avian influenza viruses in a mammalian host. PLoS Pathog. 2009
604   Dec;5(12):e1000709.

605 [50] Imai M, Yamashita M, Sakai-Tagawa Y, et al. Influenza A variants with reduced
606   susceptibility to baloxavir isolated from Japanese patients are fit and transmit through
607   respiratory droplets. Nat Microbiol. 2020 Jan;5(1):27-33.

608 [51] Kristensen C, Jensen HE, Trebbien R, et al. Avian and Human Influenza A Virus Receptors
609   in Bovine Mammary Gland. Emerg Infect Dis. 2024 Sep;30(9):1907-1911.

610 [52] Jassem AN, Roberts A, Tyson J, et al. Critical Illness in an Adolescent with Influenza
611   A(H5N1) Virus Infection. N Engl J Med. 2024 Dec 31.

612 [53] Eisfeld AJ, Biswas A, Guan LZ, et al. Pathogenicity and transmissibility of bovine H5N1
613   influenza virus. Nature. 2024 Sep 12;633(8029).

614 [54] Gu C, Maemura T, Guan L, et al. A human isolate of bovine H5N1 is transmissible and
615   lethal in animal models. Nature. 2024 Oct 28.

616 [55] Pulit-Penaloza JA, Belser JA, Brock N, et al. Transmission of a human isolate of clade
617   2.3.4.4b A(H5N1) virus in ferrets. Nature. 2024 Oct 28.

618 [56] Rosenke K, Giffin A, Kaiser F, et al. Pathogenesis of bovine H5N1 clade 2.3.4.4b infection
619   in Macaques. Nature. 2025 Jan 15.

620 [57] Garg S, Reinhart K, Couture A, et al. Highly Pathogenic Avian Influenza A(H5N1) Virus
621   Infections in Humans. N Engl J Med. 2024 Dec 31.

622 [58] Centers for Disease Control and Prevention. CDC Confirms First Severe Case of H5N1 Bird
623   Flu in the United States. https://www.cdc.gov/media/releases/2024/m1218-h5n1-
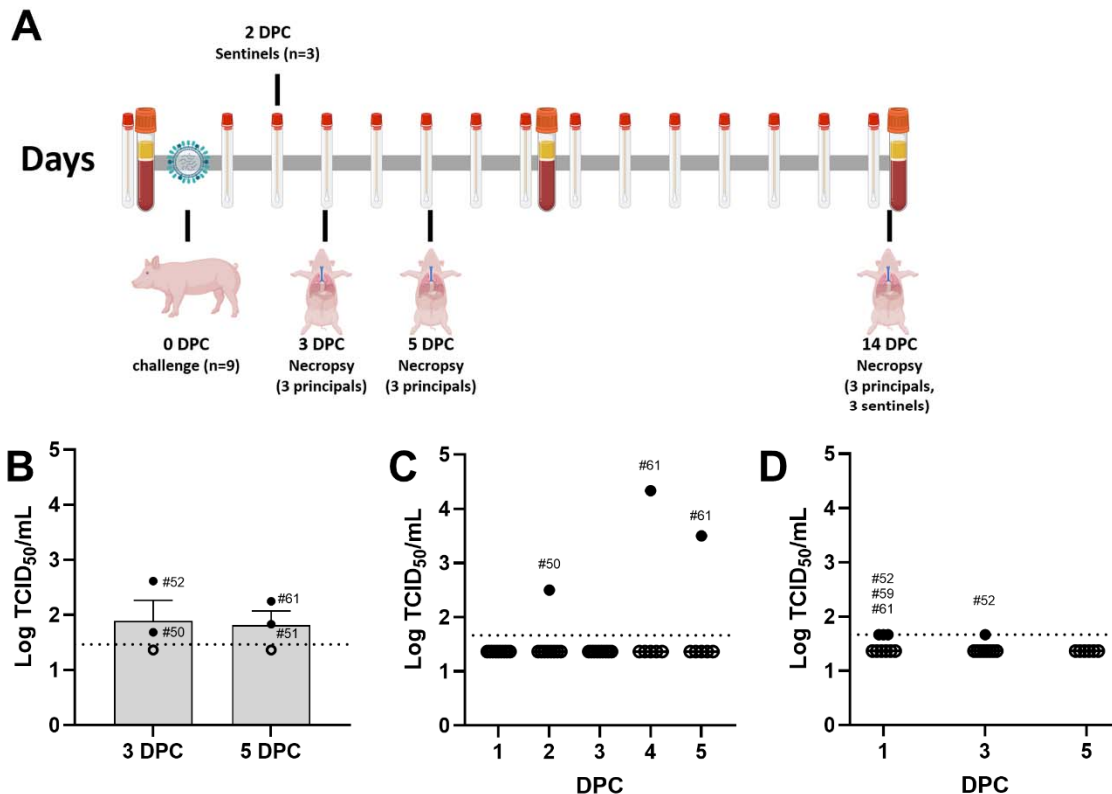624   flu.html2024.

625

626

Figure 1. Study design and virus replication in pigs infected with a bovine-derived HPAI H5N1 B3.13 virus. (A) nine principals were challenged with 5×10^6 $TCID_{50}$ per pig via intra-tracheal (2 mL), intranasal (1 mL), and oral (1 mL) routes. Three sentinels were commingled with principals in a single pen at 2 DPC. Six pigs were randomly selected and humanly euthanized at 3 (n=3, pig ID: #50, #52, and #54) and 5 DPC (n=3, #51, #53, and #61), and the remaining three principals (#57, #59, and #60) and three sentinels (#55, #56, and #58) were humanly euthanized at 14 DPC. Nasal swab, oropharyngeal swab, and serum were collected throughout the study. Nasal swab (B), and oropharyngeal swab (C), and bronchoalveolar lavage fluid or BALF (D). Virus titration was performed on MDCK cells and virus-infected cells were visualized by immunofluorescence assay. The positive samples were shown as closed circles with pig ID; open circles represent below a limit of detection. The dash line is the LOD of assay (3.29×10^1 $TCID_{50}$/mL for BALF and 4.64×10^1 $TCID_{50}$/mL for swabs).
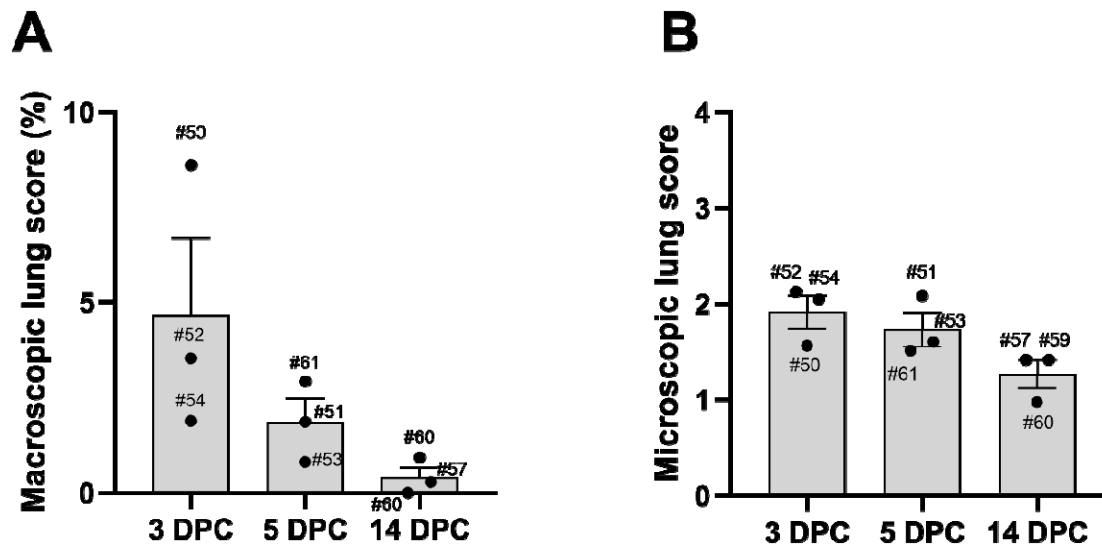
Figure 2. Macroscopic (A) and microscopic (B) lung scores in pigs infected with a bovine-derived HPAI H5N1 B3.13 virus. Macroscopic lung scores were calculated based on the percentage of the surface area showing lobular atelectasis and hyperemia. Microscopic scores were calculated by the average scores of six different criteria.
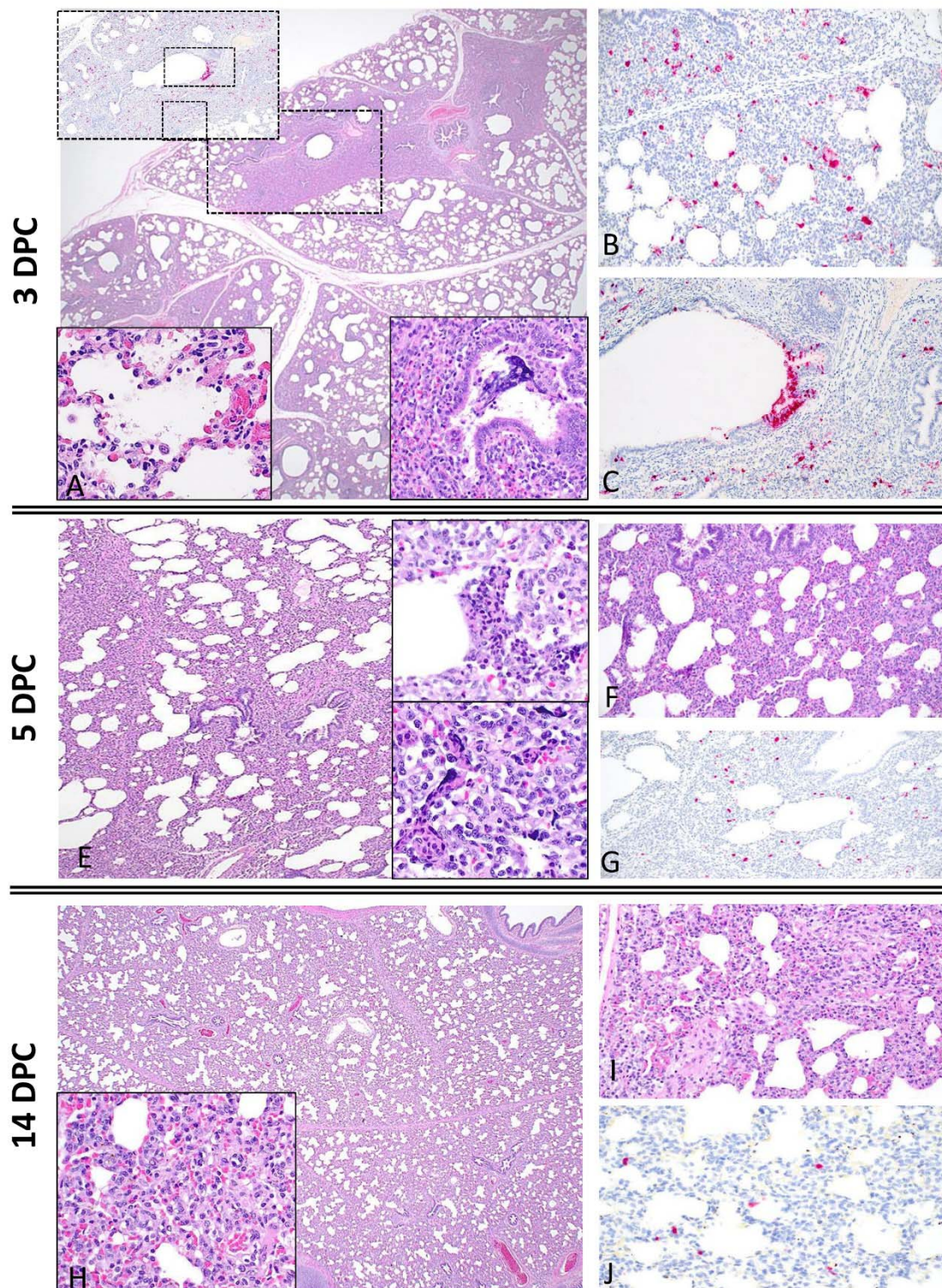
Figure 3: Histological features in lungs of pigs infected with a bovine-derived HPAI H5N1 B3.13 virus. Histologically, pulmonary lesions were characterized by multifocal to coalescing interstitial pneumonia with limited necrotizing bronchiolitis. At 3 DPC (A and lower right inset),

25 multifocal bronchopulmonary segments were characterized by infrequent bronchiolar epithelial
26 cell degeneration and necrosis (lower right inset) and associated areas of pulmonary parenchyma
27 with collapsed alveolar spaces (atelectasis) and expanded alveolar septa by lymphocytes and
28 histiocytes (A) and alveolar epithelial necrosis (A-lower right inset). Influenza A virus
29 nucleoprotein intracytoplasmic antigen was detected within pneumocytes and alveolar
30 macrophages (B) and segmentally or individually within bronchiolar epithelial cells (C).
31 Infrequent yet similar epithelial necrosis was noted at 5 DPC (E, upper and lower insets), which
32 is accompanied by multifocal to coalescing interstitial pneumonia characterized by alveolar
33 septal thickening and cellular debris filling alveolar spaces (E and F) (F). Influenza A virus
34 nucleoprotein antigen was much less abundant and mostly in cells lining and within alveoli (G).
35 At 14 DPC, there are multifocal to coalescing regions areas of mild to moderate interstitial
36 pneumonia. Alveolar septa are thickened by infiltrates of lymphocytes and macrophages and
37 there is multifocal thickening of lobular septa with non-suppurative inflammation (H asterisk and
38 I). Sporadic epithelial cells in bronchioles and alveoli as well as septal macrophages contained
39 viral antigen (J). Magnifications of images: 20× for A, E and H, 100× for B, C, F, G, I and J.
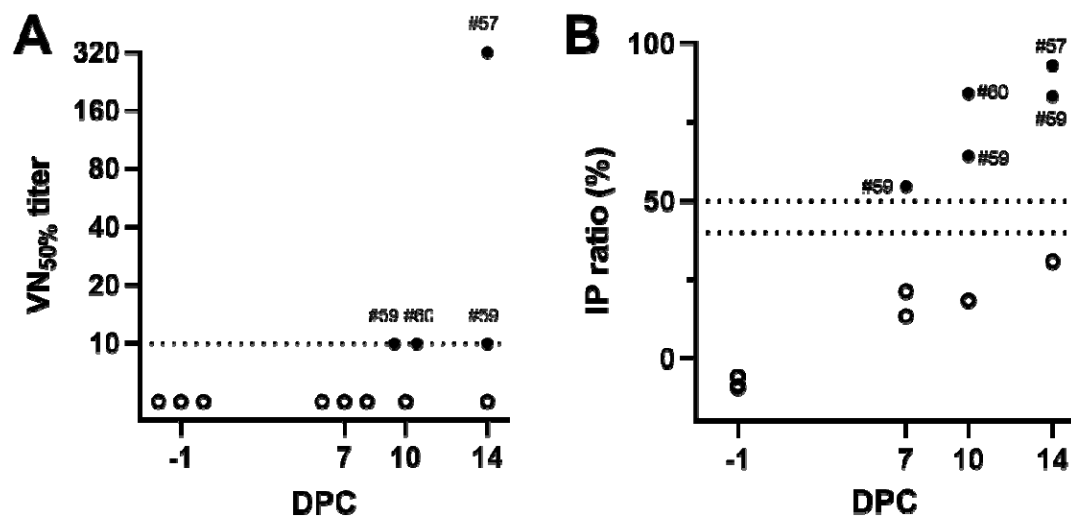40 Magnifications of inserts: 400× for A, E and H and 100× for lower right (A).

41

Figure 4. Antibody responses in pigs infected with a bovine-derived HPAI H5N1 B3.13 virus. Virus neutralization (VN) test (A) and commercial NP-based competition ELISA (B). (A) The virus neutralization test was performed with the challenge strain on MDCK cells to determine the 50% inhibition of virus growth. (B) Commercial NP-based competition ELISA (BioStone, USA) was used to determine serological responses. The positive samples were shown as closed circles with pig ID: open circles represent negative. The dash line is the initial dilution for the VN test (1:10) and the cut-off value of ELISA, <40%: negative, 40-50%: doubtful, >50% positive.
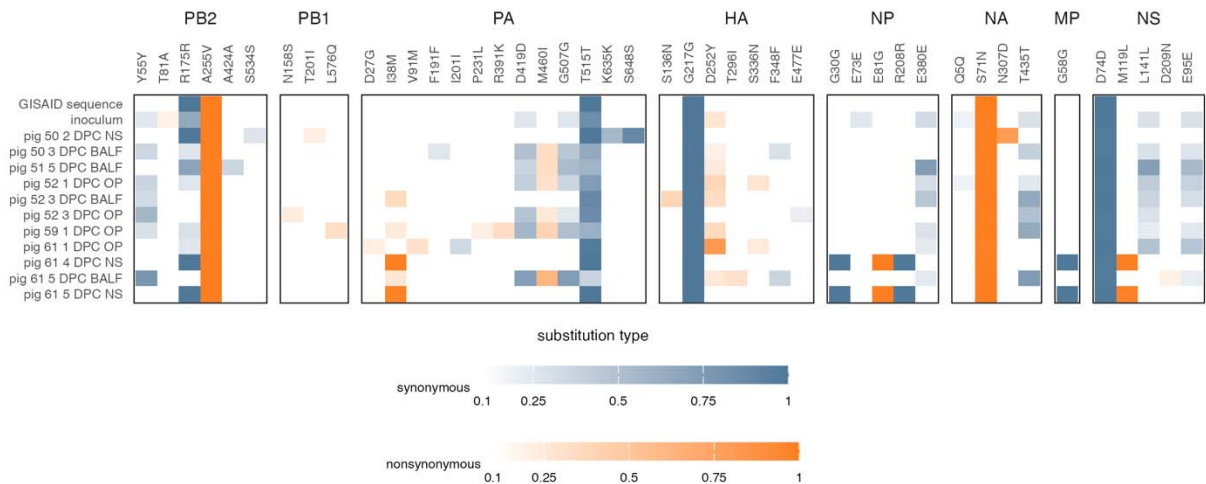
Figure 5. Consensus and subconsensus-level variants across the influenza virus genome in pigs infected with a bovine-derived HPAI H5N1 B3.13 virus. Nonsynonymous and synonymous variants are shown in relation to our analytical pipeline's standard reference sequence, A/Bovine/Texas/24-029328-01/2024. Amino acid location and identity are labeled. We used the isolate A/Cattle/Texas/063224-24-1/2024 (EPI_ISL_19155861) in this study. The original cattle isolate sequence as deposited in GISAID (GISAID sequence) and the virus stock used to inoculate pigs (inoculum) are also shown in the figure. The inoculum was propagated on bovine uterine epithelial cells for 3 passages at Cornell University and then propagated on MDCK cells for 1 passage at Kansas State University prior to inoculating animals in this study. NS=nasal swab, BALF=bronchoalveolar lavage fluid, and OP=oropharyngeal swab.